A pharmacokinetic study of DNA minor groove binding pyrrole-imidazole polyamide: a correlation between its physicochemical property and the *in vivo* distribution in tumor-bearing mice

(DNA 結合性ポリアミドの物理化学的特性と腫瘍組織集積性に関する薬物動態学的検討)

千葉大学大学院医学薬学府

先端医学薬学専攻

（主任　：　永瀬 浩喜教授）

井上貴博

Contents

1. Abstract

Objective: Pyrrole-imidazole (PI) polyamide is a class of compounds consisting of *N*-methylpyrrole (Py) and *N*-methylimidazole (Im), which is able to bind to the minor groove of double-stranded DNA in a sequence-specific manner. PI polyamide is considered to be an attractive compound for anti-tumor drug development because of its tumor-targeting property; however, its molecular mechanism(s) remains largely elusive. The primary structure of PI polyamide might affect its physicochemical property and thereby influencing its biodistribution. In the present study, we examined the effects of chemical composition of PI polyamide on its tumor accumulation *in vivo*.

Methods: PI polyamide-fluorescein conjugates with the distinct number of Im units were synthesized by a solid-phase peptide synthesis. The degree of hydrophobicity was determined by the retention time of high performance liquid chromatography. The biodistribution of these compounds in xenograft tumor-bearing mice was analyzed by an *in vivo* fluorescence imaging system.

Results: There existed an inverse relationship between the number of Im rings of the compounds and the degree of hydrophobicity. All compounds accumulated rapidly within xenograft tumors regardless of their primary structures. Highly hydrophobic compounds showed long-term retention in tumor tissues compared to less hydrophobic

compounds. Additionally, hydrophobic compounds accumulated mainly in livers, while less hydrophobic compounds detected predominantly in kidneys.

Conclusion: The present results suggest that the composition of PI polyamide, which contributes to its hydrophobic property, has an implication for its accumulation and retention in tumor tissues *in vivo*.

2. Introduction

Pyrrole-imidazole (PI) polyamide is a class of compounds consisting of *N*-methylpyrrole (Py) and *N*-methylimidazole (Im) aromatic amides originally derived from natural oligopeptide antibiotics, such as distamycin A. While distamycin A non-covalently binds to the minor groove of adenine (A) and/or thymine (T) -rich DNA sites,[1] PI polyamides possess a similar specificity for nucleotide binding and improved base recognition, where Im recognizes guanine (G) and Py binds to A, T, and cytosine (C).[2-4] PI polyamide physically associates with the minor groove of double-stranded DNA without distorting the helical structure, especially in a γ-aminobutyric acid-linked hairpin configuration.[5] This class of molecules affords binding affinities comparable to certain transcription factors.[6] As such, well-designed PI polyamides targeting to promoter and enhancer elements of the genes of interested could interrupt the assembly of transcription factors, such as TFIIIA,[7] AP-1,[8, 9] and HIF-1,[10] and thereby repressing its gene expression.

As aberrant gene expressions as a result of genetic and epigenetic abnormalities have been well implicated in various diseases, the use of PI polyamides presents an attractive option for the development of novel drugs against those diseases. Recently, a PI polyamide targeting to the promoter of *TGFB1* successfully ameliorated progressive

renal diseases[9] and hypertrophic scars.[11] Another PI polyamide against an androgen receptor responsible element (ARE) was able to repress the ARE-regulated gene transcriptions, e.g. *VEGF* and *TMPRSS2-ERG*, a unique prostate cancer-related oncogenic fusion gene, and thereby suppressing the xenograft tumor growth of human prostate cancer cells.[12, 13] Our recent study of a PI polyamide against oncogenic driver mutant genes $KRAS^{G12D/V}$ demonstrated differential cytotoxicity *in vitro* and repressed tumor growth in mouse xenograft models *in vivo* without severe adverse effects such as body weight loss,[14] highlighting the promising aspect of PI polyamides in drug development.

While the ability for PI polyamides to accumulate in certain tissues has been revealed in several studies, the underlying physiochemical principles remain unclear. Recent studies showed PI polyamides to accumulate into skin xenograft tumors[15, 16] and vital organs such as liver, kidney, and lung,[17] but so far there are few explanations for such a phenomenon. Previously, Fukasawa *et al*. proposed that the plasma level of intravenously administrated PI polyamide increased positively as their molecular weight,[18] and Kamei *et al*. hypothesized a potential connection between the Py/Im ratio of a polyamide and its plasma level *in vivo*.[19] As results from Best et al. echoed similar sentiments to the hypothesis that the primary structure of a PI polyamide affected a

molecule's distribution *in vivo*, we sought to characterize the potential connection here, as few studies have systematically examined the biodistribution of PI polyamides *in vivo*[20] and no general design roles on how to utilize the pharmacokinetic profiles of PI polyamides to improve its accumulation/retention, biological elimination and organ/tissue distribution for therapeutic puroposes.

In the present study, we have designed a series of hairpin ten-ring PI polyamides with distinct ratios of Py and Im units to infer the possible effect of hydrophobicity, as governed by the number of Im units, on the molecular machinery of their internalization into tumor tissues *in vivo*. While all PI polyamides rapidly accumulated into tumor tissues, PI polyamides with higher Im unit numbers displayed longer retention times in tumor tissues compared to their counterparts with lower Im unit numbers, suggesting that the primary structure of PI polyamide did in fact affect its tissue distribution *in vivo*. Thus, the hydrophobic property of PI polyamide or other properties resulting from its chemical compositions might be implicated in its pharmacodynamic properties.

3. Materials and Methods

3.1 General materials

Human colon cancer-derived cell lines LS180 and SW480 were obtained from American Tissue Culture Collection (Manassas, VA, USA). PyBOP and NovaPEG Wang resin were acquired from Novabiochem (Gibbstown, NJ, USA); unless otherwise specified, chemicals were obtained from Sigma-Aldrich (St. Louis, MO, USA).

3.2 Chemical synthesis of pyrrole-imidazole (PI) polyamide-fluorescein conjugates

Compounds **1**-**5** were piecewise synthesized by first generating the polyamide backbone chains (**1**, β-PyIm-β-PyPyPy-γ-PyPyPy-β-PyPy; **2**, β-ImIm-β-PyPyPy-γ-PyPyPy-β-PyPy; **3**, β-ImIm-β-ImPyPy-γ-PyPyPy-β-PyPy; **4**, β-ImIm-β-ImImPy-γ-PyPyPy-β-PyPy; **5**, β-ImIm-β-ImImIm-γ-PyPyPy-β-PyPy) by stepwise Fmoc solid-phase reaction using a PSSM-8 solid-phase peptide synthesizer (Shimadzu Industry, Kyoto, Japan) at 10 μmol scales of Fmoc-β-alanine NovaPEG Wang resin as previously described.[39] After the synthesis, *N*, *N*-Dimethyl-1, 3-propanediamine (Wako, Tokyo, Japan) was mixed with the resin at 65 ºC for 2 hours for compound cleavage. PI polyamides having the carboxyl-terminal amine was purified

by a Prominence high-performance liquid chromatography (HPLC) (Shimadzu Industry, Kyoto, Japan) using a 10 mm×150 mm Gemini-NX3u 5-ODS-H reverse-phase column (Phenomenex, Torrance, CA, USA) in 0.1% acetic acid in water with acetonitrile as eluent, at a flow rate of 10 mL/minute, and a linear gradient from 0% to 66.7% acetonitrile over 20 minutes, with ultraviolet detection at 310 nm. Collected polyamide backbones were conjugated with fluorescein as previously described.[20] In brief, the polyamides were dissolved in *N*-methylpyrrolidone with fluorescein-4-Isothiocyanate (FITC; 5 equivalents, Dojindo, Kumamoto, Japan) and *N*, *N*-Diisopropylethylamine (10 equivalents, Wako, Tokyo, Japan). After reaction at room temperature for 2 hours, the resulting polyamide-fluorescein conjugates were purified by HPLC as described conditions and analyzed by an LCMS-2020 liquid chromatograph mass spectrometer (LC MS) system (Shimadzu Industry, Kyoto, Japan) using a 150 x 4.6 mm Gemini-NX 3u 11A reverse-phase column (Phenomenex, Torrance, CA, USA). **1**: LC-MS *m/z* calculated for $C_{101}H_{111}N_{29}O_{20}S$, $[M+2H]^{2+}$ 1041.92; found 1042.25, $[M+3H]^{3+}$ 694.94; found 695.15. **2**: LC-MS *m/z* calculated for $C_{100}H_{110}N_{30}O_{20}S$, $[M+2H]^{2+}$ 1042.41; found 1042.90, $[M+3H]^{3+}$ 695.27; found 695.55. **3**: LC-MS *m/z* calculated for $C_{99}H_{109}N_{31}O_{20}S$, $[M+2H]^{2+}$ 1042.91; found 1043.40, $[M+3H]^{3+}$ 695.61; found 695.95. **4**: LC-MS *m/z* calculated for $C_{98}H_{108}N_{32}O_{20}S$, $[M+2H]^{2+}$ 1043.41; found 1043.85, $[M+3H]^{3+}$ 695.94;

found 696.25. **5**: LC-MS *m/z* calculated for $C_{97}H_{107}N_{33}O_{20}S$, $[M+2H]^{2+}$ 1043.91; found 1044.30, $[M+3H]^{3+}$ 696.27; found 696.55.

3.3 Estimation of logP_{OW} value

The logP_{OW} values were estimated by using reverse-phase HPLC as previously described[40]. In brief, retention times of compounds were measured by using a Prominence HPLC system (Shimadzu Industry, Kyoto, Japan) using a 150 x 4.6 mm Gemini-NX 3u 11A reverse-phase column (Phenomenex, Torrance, CA, USA) with performed in an isocratic condition (0.1% acetic acid : acetonitrile = 4 : 1) at a flow rate of 1 mL/minute. A standard curve was constructed by plots of the logP_{OW} values versus retention times of reference substrates, such as ethyl acetate,[41] benzonitrile,[41] acetophenone[41] and indole[42], and then logP_{OW} values of PI polyamides were estimated by their retention times.

3.4 Fluorescence quantum yield

Fluorescence spectra were measured by an FP-8600 spectrometer (JASCO, Tokyo, Japan) and corrected with correlation functions for excitation and mission optics

obtained by use of an SID-844 calibration detector (JASCO, Tokyo, Japan). Absorption spectra were recorded by a UV-2400PC spectrometer (Shimadzu Industry, Kyoto, Japan).

Fluorescence quantum yield ($\emptyset_f$) was estimated by the relative method using a formula,

$$\emptyset_f = \emptyset_s \times \left(\frac{F_x/A_x}{F_s/A_s} \right) \times \left(\frac{n_x^2}{n_s^2} \right)$$

in which, $\emptyset$, F, A, and n are the quantum yield, the integrated fluorescence intensity, the absorbance at excitation wavelength, and the refractive index of solvent used, respectively, and subscript x and s stand for sample of interest and standard sample, respectively. Fluorescein in 1 mM NaOH/EtOH was used as standard sample ($\emptyset_f$ = 0.92).[43]

3.5 *In vitro* experiments

Human colon cancer-derived LS180 and SW480 cells were maintained with minimum essential medium (MEM, Gibco Life technology, Carlsbad, CA, USA) and Dulbecco's modified eagle medium (DMEM, Wako, Osaka, Japan) supplemented with

10 % heat-inactivated fetal bovine serum (FBS; Invitrogen, Carlsbad, CA, USA) and 50 μg/ml penicillin/streptomycin (Sigma-Aldrich, St. Louis, MO, USA) in a humidified atmosphere with 5 % CO2 at 37 °C.

For *in vitro* PI polyamide incorporation analysis, human colon cancer cells (1 x 10^5 cells) were grown on glass coverslips and treated with 1 μM of each compound for 2 hours. Cells were then washed twice with ice-cold PBS and fixed with 100% methanol for 20 minutes at -20 °C. Coverslips were mounted with VECTACHIELD Mounting Hard Set Medium with DAPI (Invtitrogen, Carlsbad, CA, USA). Fluorescence images were observed under a DMI 4000B confocal laser microscope (Leica Microsystems, Wetzlar, Germany).

For *in vitro* fluorospectrometric analysis, human colon cancer cells (1 x 10^4 cells) were treated with compounds **1**, **3**, and **5** at the indicated doses for 24 hours. Cells were washed twice in PBS. Fluorescence intensity was determined by an ARVO X-3 fluorescence spectrometer (Perkin Elmer, Franklin Lakes, NJ, USA).

3.6 Animal experiments

3.6.1 Ethics statement

Procedures involving animals outlined in the following section satisfied guidelines described in the Proper Conduct of Animal Experiments as defined by the Science Council of Japan. Approval from the Animal Care and Use Committee on the Ethics of the Chiba Cancer Center Institute was obtained prior to experimentation. All experimental steps were carefully performed to ensure the subjects endured minimal suffering.

3.6.2 Xenograft tumor model

Human colon cancer-derived LS180 (3×10^6 cells/mouse) were maintained as described above and subcutaneously inoculated into left flanks of 5- to 8-weeks female BALB/c nude mice (Oriental Yeast, Tokyo, Japan). Compounds **1**, **3**, **5**, or FITC (1 mg/kg), or DMSO/PBS (1.25%, v/v) was intravenously administrated into the tumor-bearing mice when the long diameter of xenograft tumors reached about 1 cm. Fluorescence images of the whole mice were captured at the indicated time points post-administration and the fluorescence intensity of tumor and non-tumor areas were analyzed on a Lumazone imaging system (Roper Bioscience, Tucson, AZ, USA).

For detection of compounds **1**, **3**, and **5** in tissues, the mice were sacrificed at 3 days or 9 days after administration for resection of the following tissues: tumor, liver, kidney, heart, lung, spleen, and brain were resected. Frozen sections were prepared and

observed under a DMI 4000B confocal laser microscope (Leica Microsystems, Wetzlar, Germany). Mean fluorescence intensity of tissue sections obtained from the PI polyamide-treated mice (n = 3) was determined by using a WinROOF version 7.0 software (Mitani Corporation, Tokyo, Japan).

3.7 Statistical analysis

Results were presented as mean ± SD of three independent experiments. Data were compared using the unpaired *t*-test, one-way ANOVA, and repeated-measure two-way ANOVA by Ekuseru-Tokei 2010 software (Social Survey Research Information Co., Ltd., Tokyo, Japan) and p-value < 0.05 was considered to be significant.

4. Results

4.1 Molecular design and synthesis of PI polyamide-fluorescein conjugates

To examine whether the compositional variation of PI polyamides could affect its hydrophobicity, we designed five PI polyamide-fluorescein conjugates with different compositions of Im units: **1**-**5** (Figure 1). Im units were located at positions 1 through 7 in hairpin configurations to avoid Im/Im pairings as previous studies suggested that such pairing had no preferential affinity for G-C or A-T pairs.[3] According to the previous studies, β-alanine (β) and γ-aminobutyric acid (γ) residues were incorporated in order to allow the polyamides to be flexible and the hairpin-like structure, respectively.[5, 21, 22] The designed PI polyamide–fluorescein conjugates **1**–**5** were synthesized via the Fmoc solid-state peptide synthesis procedure followed by a conjugation of fluorescein with PI polyamides at their N-termini as described in Materials and Methods. Purities (> 96%) of the resulting PI polyamide–fluorescein conjugates were confirmed by a high performance liquid chromatography (HPLC), and these compounds were used for following experiments (Figure 2).

4.2 The number of imidazole units of PI polyamide reflects its hydrophobicity

A molecule's equilibrium partitioning in a biphasic water and *n*-octanol system, as determined by its logP_{OW}, is a common indicator for the hydrophobicity, measureable from their HPLC corresponding retention times.[23] We thereby measured the retention times of compounds **1**-**5** and reference compounds, such as ethyl acetate, benzonitrile, acetophenone, and indole (Figure 3), and likewise deduced the logP_{OW} values of **1**-**5** from their recorded retention times (Table 1). Compound **1** with only one Im unit exhibited the highest logP_{OW} value, while **5** with five Im units showed the lowest the logP_{OW} value among these compounds. In addition, the logP_{OW} values of **2**-**4** were gradually reduced along with the increase in the number of Im units. These results suggested a clear inverse correlation between logP_{OW} values of compounds **1**-**5** and their respective number of Im units.

In the meantime, we analyzed the fluorescence of each polyamide as a precaution to confirm that fluorescence of fluorescein moiety did not vary resulting from a function of the chemical structure of the PI polyamide adduct. We saw an increase in the level of fluorescence quantum yield of compounds **1**-**3** with their Im unit numbers; however, it was decreased in compounds **4** and **5** (Table 1). Consistently, compounds **1**, **2** and **5** displayed similar fluorescence, while **3** and **4** had the highest and the lowest

fluorescence intensity, respectively (Figure 4). Because **4** showed the lowest fluorescence intensity and hydrophobicity of **2** was similar to **1**, we employed three compounds for further experiments: **1** as a highly hydrophobic compound, **3** as a moderately hydrophobic compound, and **5** as a relatively hydrophilic compound.

4.3 A mode of internalization of PI polyamide-fluorescein conjugates into tumor-derived cells

We next examined the incorporation of PI polyamide-fluorescein conjugates by tumor-derived cells *in vitro* by fluorescent microscopy. Human colon cancer LS180 and SW480 cells were treated with **1**, **3**, and **5** followed by 4′, 6-diamidino-2-phenylindole (DAPI) staining. Consistent with previous studies,[8, 20, 24] **1**, **3**, and **5** strongly co-localized with DAPI, indicating that these compounds highly accumulated in cell nuclei regardless of the distinct hydrophobicity (Figure 5a and 5b). Fluorescein was undetectable in the cells (Figure 5a and 5b).

We further investigated how PI polyamide-fluorescein conjugates is incorporated by cells. LS180 and SW480 cells were treated with various concentrations of compounds and measured fluorescence intensity by a fluorescence spectrometer. As seen in Figure

5c and 5d, **1** was internalized into LS180 and SW480 cells in a dose-dependent manner, whereas the dose dependency was not seen in **3** or **5**. These data suggested that hydrophobic PI polyamides were likely incorporated by tumor-derived cells through passive diffusion instead of other possible transport mechanisms.

4.4 Accumulation of hydrophobic PI polyamides into tumor *in vivo*

To test whether the hydrophobicity of compounds **1**, **3**, and **5** could affect its tumor-oriented distribution *in vivo*, we intravenously injected **1**, **3**, **5**, alongside unconjugated fluorescein or dimethyl sulfoxide (DMSO) as controls, into nude mice bearing LS180-derived tumors. The superficial fluorescence of these mice was monitored for 72 hours post-administration by quantitative *in vivo* imaging; the mean fluorescence intensity (MFI) in tumor and in non-tumor area was summarized in Figure 6. In the tumor area, **1** showed an increase in the level of MFI with a peak at 3 hours post-administration that sustained over 72 hours (Figure 6a and 6f). Compound **3** also had an elevated MFI in tumors with a peak at 6 hours post-administration, and nearly half of its maximum level was still detectable at 72 hours post-administration (Figure 6b and 6g); the MFI of **5** in the tumors reached its maximal level at 3 hours post-administration and it became undetectable at 48 hours post-administration (Figure

6c and 6h). In contrast, we could not detect fluorescence in the tumor tissues of subjects injected with unconjugated fluorescein, despite that it did appear to distribute in the entire body with similar kinetics to that of **3** (Figure 6d and 6i). This observation affirmed that the fluorescence observed in the tumor tissues of polyamide-injected mice was in fact due to the conjugated fluorescein moiety on the polyamides. Beyond the graft regions, **1** rapidly distributed in the body cavity within 1 hour, and its level sharply decreased at 24 hours post-administration (Figure 6a and 6f), whereas **3** experienced a spike in MFI in non-tumor areas within 5 minutes but disappeared at 24 hours post-administration (Figure 6b and 6g). The level of **5** was almost undetectable in the entire body during the experiment (Figure 6c and 6h). Similar proportion of distribution of PI polyamide-fluorescein conjugates was seen in another human colon cancer SW480-derived tumor bearing mice (Figure 7), collectively suggesting that hydrophobicity of PI polyamide influences tumor-oriented distribution.

4.5 Long retention of hydrophobic PI polyamides within tumor *in vivo*

Since the half level of **1** and **3** in the tumor seemingly extended beyond 3 days after their initial injections, we further investigated long-term retention of PI polyamide-fluorescein conjugates in tumor-bearing mice. To this end, we treated the

LS180-bearing nude mice with compounds **1**, **3**, and **5** and monitored the resultant fluorescent decay by quantitative *in vivo* imaging until their fluorescein signal was disappeared (Figure 8). The fluorescence of compounds **1**, **3**, and **5** reached their maximal levels around 2 hours post-administration and decreased by half around 48 hours post-administration. Surprisingly, **1** was still detectable in tumors over 9 days post-administration, while **3** did not; additionally, we found the fluorescence of **5** to extinguish in a time frame as short as 4 days. Notably, **1** was detectable within SW480-derived tumors *in vivo* for up to 22 days (Figure 9), indicating that increasing the hydrophobicity or other properties of the PIP likely contributed to a longer tumor retention time *in vivo*.

4.6 Tissue distribution of hydrophobic PI polyamides

The results so-far prompt us to analyze further the distribution of PI polyamide-fluorescein conjugates in tissue sections. PI polyamide-fluorescein conjugates-inoculated animals were resected at 3 days and 9 days post-administration, and the tissue fluorescence distribution was assessed by confocal microscopy. Compounds **1, 3**, and **5** were mainly detectable in tumors, livers and kidneys at 3 days post-administration, and appeared to co-localize with DAPI, implying that PI

polyamide-fluorescein conjugates accumulated in the nucleus *in vivo* (Figures 10-12). There was no fluorescence in any of the regions tested in DMSO-treated mice (Figure 13). We further measured the MFIs in these tissue sections. As shown in Figure 14a, **1** accumulated preferentially in tumors, and the liver to a smaller extent, and poorly presented in the kidney and spleen on 3 days post-administration. At the same time, **3** was detected in tumors as well as kidneys, but accumulation in the liver was relatively low (Figure 14b). Compound **5** was largely detected in kidneys compared to tumors and livers (Figure 14c). Compound **1** remained notably detectable in tumor at 9 days post-administration (Figure 14a). In contrast, levels of **3** and **5** in tumor tissues largely decreased at 9 days post-administration (Figures 14b and 14c), suggesting that the hydrophobic property influences the biodistribution of PI polyamides *in vivo*.

5. Discussion

5.1 Effect of chemical structure of PI polyamide on its hydrophobicity

We herein have synthesized a series of PI polyamides **1**-**5** with different number of Im units to confer the distinct hydrophobicity. Given that the presence of an additional nitrogen atom of Im affected its propensity for hydrogen bonding, the degree of hydrophilicity of Im (logP_{OW} = -0.06) is larger than that of Py (logP_{OW} = 1.21)[25, 26]. In comparison with their logP_{OW} values, the hydrophobicity of **1** was approximately twice higher than that of **5**. Thus, the hydrophilic level of PI polyamide might be correlated with the number of Im units. In this study, all of Im units were located at the positions before the γ unit of compounds **1**-**5** to simplify their chemical structure. According to the extensive studies as reviewed,[27] the position of Im unit served a critical role in the specificity of PI polyamide for the recognition of DNA; thereby, their positions would be scattered throughout the molecule in a nucleotide-sequence dependent manner. It was possible that the different composition of Im units could influence the hydrophobicity of PI polyamide despite the same numbers of Im units; therefore, the measurement of logP_{OW} by using HPLC should be required for the development of PI polyamide-based medicine.

5.2 Effects of hydrophobic structures of PI polyamides on tumor-oriented accumulation and retention

In the present study, we demonstrated for the first time that the retention time of PI polyamide in tumor tissue was inversely correlated with its Im unit numbers: compound **1** with only one Im unit was detectable within tumor tissues longer than **3** with three Im units, whereas **5** with five Im units could no longer be found after 3 days. Additionally, **1** retained in tumors over 22 days, a longer retention time compared to previous studies.[15] Similarly, the most hydrophobic **1** was delivered into tumor tissues much higher than compounds **3** and **5**. Because the fluorescence intensities of compounds **1**, **3**, and **5** were nearly equal, we speculated that the hydrophobic level of PI polyamides is involved in its tumor-oriented delivery.

Tumor cells activated tumor-associated angiogenesis upon the deprivation of oxygen and nutrients accompanying the tumor growth, and thereby accelerating growth of tumor tissues.[28] Raskatov *et al*. demonstrated an increased accumulation of PI polyamides in tumors *in vivo* as a function of relationship between xenograft host and tumor tissue, such as tumor vascularization.[29] It has been considered that tumor vascular system is different from blood vessels in normal organs, such as defective vascular architecture and deficiency of lymphatic drainage from tumor tissue.[30] Additionally,

many kinds of macromolecules like plasma proteins as well as lipids predominantly accumulated and retained in tumor tissues, so-called the enhanced vascular permeability and retention (EPR) effect.[31, 32] As Chenoweth *et al*. demonstrated that certain PI polyamides strongly bind to plasma proteins,[33] we hypothesized that the Im unit numbers of PI polyamide, which partly contributes to the degree of hydrophobicity, would have an impact on its association with plasma proteins or lipids, resulting in its accumulation into tumor tissue, at least in part mediated by the EPR effect. Our histological examination supported a similar notion that the hydrophobic PI polyamide **1** in tumor tissue was distributed by the surrounding blood vessels (Figure 15); however, more detail analysis of the binding affinities of PI polyamides to plasma proteins and the relationship between hydrophobicity of PI polyamides and histological distribution in tumor tissues would need to be clarified.

We also have demonstrated for the first time that the mode of internalization of PI polyamide into tumor-derived cells is associated with the Im unit numbers. Because of a dose dependent internalization of **1**, hydrophobic PI polyamide might penetrate into cells within tumor tissues through the passive diffusion. In contrast, certain transport systems could be involved in the incorporation of relatively hydrophilic **3** and **5**. Since certain mechanisms to uptake extracellular substrates were activated in tumor cells via

oncogenic signaling pathway,[34] it could be possible that higher activation of endocytosis in tumor cells is responsible for the higher uptake of PI polyamides compared to normal organs. However, further examination to uncover how the tumor cells incorporate PI polyamides remains to be elucidated.

5.3 A hydrophilicity-mediated distribution and excretion of PI polyamide

Another important finding of the present study was the effect of the hydrophobicity of a PI polyamide's biodistribution *in vivo*. Consistent with previous studies,[15, 29, 35] the hydrophobic **1** was preferentially delivered into livers as well as tumors; however, the hydrophilic **5** was predominantly accumulated in kidneys. Our *in vivo* imaging analysis also demonstrated that hydrophilic **5** was rapidly cleared from the body relative to the hydrophobic **1** and **3**, suggesting that the serum/tissue half-life of PI polyamides *in vivo* is associated with its hydrophilicity.

Various drugs are eliminated from the body by renal and/or bile excretion. Harki *et al*. described that a hairpin-formed PI polyamide would firstly be transported in the liver and then delivered into bladder rather than gallbladder, implying a possible mode of renal excretion.[35] We saw a rapid decrease in the circulation level of **5** at an earlier time

point than that of **1** and **3**. As the fluorescence intensity of **1**, **3**, and **5** was nearly equal, the likely explanation was that an increase in the hydrophilic level of PI polyamide elevates the rate of its renal excretion as a result of "kidney-homing". Intriguingly, the moderately hydrophobic **3** was observed in both tumors and kidneys, and remained in tumors longer than **5**, suggesting that the hydrophilicity of a PI polyamide contributed to its tumor-homing but not liver-homing property *in vivo*. In support of our hypothesis, Synold *et al*. also demonstrated that acetylating PI polyamide could potentially increase its hydrophobicity to the extent of altering localization in tissues such as livers, kidneys and lungs and rapidly reducing its plasma concentration.[36] Additionally, several chemical modifications at γ-turn[37] and PEGylation at the carboxyl terminus[38] affected the hydrophobicity of PI polyamide. Thus, an increase in the hydrophilic level of PI polyamide might reduce adverse effect of PI polyamide-based medicine resulting from the modulation of biodisribution *in vivo*, especially the reduction of "liver-homing" property.

6. Conclusion

PI polyamides with different Im unit numbers were synthesized and examined for their differences in tissue distribution within tumor bearing mice. The Im unit numbers of PI polyamides were contributed to a polyamide's hydrophobicity in a manner that affected its accumulation and retention in tumor tissues as well as its internalization into tumor-derived cells *in vitro*. Intriguingly, we found that moderately hydrophobic PI polyamides decline the ability of "liver-homing" compared to highly hydrophobic polyamides, suggesting that well-designed PI polyamides potentiate the "tumor-homing" ability and can be utilized as a novel drug delivery system to reduce adverse effects to unintended regions of the body.

7. Acknowledgement

I would like to express the deepest appreciation to Professor Hiroki Nagase (Graduate school of Medical and Pharmaceutical Sciences, Chiba University) for his affectionate guidance. I am grateful to Dr. Osamu Shimozato (Senior Investigator of laboratory of DNA Damage Signaling in Chiba cancer center research institute) for assistance and warmful encouragements. I appreciate the feedback offered by present members and alumni of laboratories of Cancer Genetics, Innovative Cancer Therapeutics, and DNA Damage Signaling in Chiba cancer center research institute. I also thank Yusei Suzuki for technical assistance and Professor Joe Otsuki (Department of materials and Applied Chemistry, College of Science and Technology, Nihon University) for help in measurement of fluorescence quantum yield. This work was supported in part by grants-in-aids for Scientific Research (B), for Scientific Research (C), for AMED (Japan Agency for Medical Reseach and Development), for JSPS Fellows from Japan Society for the Promotion of Science (Grant numbers: JP17H03602, JP16K10559, 17ck0106356h0001, JP16J05439, respectively) and The Yasuda Medical Foundation. I thank the JSPS for a Research Fellowship for Young Scientist (DC2).

8. References

1. J.G. Pelton, D.E. Wemmer. *Proc Natl Acad Sci U S A*, **1989**, 86 : 5723.
2. M. Mrksich, W.S. Wade, T.J. Dwyer, B.H. Geierstanger, D.E. Wemmer, P.B. Dervan. *Proc Natl Acad Sci U S A*, **1992**, 89 : 7586.
3. S. White, E.E. Baird, P.B. Dervan. *Chem Biol*, **1997**, 4 : 569.
4. C.L. Kielkopf, E.E. Baird, P.B. Dervan, D.C. Rees. *Nat Struct Biol*, **1998**, 5 : 104.
5. M. Mrksich, M.E. Parks, P.B. Dervan. *J Am Chem Soc*, **1994**, 116 : 7983.
6. J.W. Trauger, E.E. Baird, P.B. Dervan. *Nature*, **1996**, 382 : 559.
7. J.M. Gottesfeld, L. Neely, J.W. Trauger, E.E. Baird, P.B. Dervan. *Nature*, **1997**, 387 : 202.
8. X. Wang, H. Nagase, T. Watanabe, H. Nobusue, T. Suzuki, Y. Asami, Y. Shinojima, H. Kawashima, K. Takagi, R. Mishra, J. Igarashi, M. Kimura, T. Takayama, N. Fukuda, H. Sugiyama. *Cancer Sci*, **2010**, 101 : 759.
9. H. Matsuda, N. Fukuda, T. Ueno, M. Katakawa, X. Wang, T. Watanabe, S. Matsui, T. Aoyama, K. Saito, T. Bando, Y. Matsumoto, H. Nagase, K. Matsumoto, H. Sugiyama. *Kidney Int*, **2011**, 79 : 46.
10. Y. Kageyama, H. Sugiyama, H. Ayame, A. Iwai, Y. Fujii, L.E. Huang, S. Kizaka-Kondoh, M. Hiraoka, K. Kihara. *Acta Oncologica*, **2006**, 45 : 317.
11. H. Washio, N. Fukuda, H. Matsuda, H. Nagase, T. Watanabe, Y. Matsumoto, T. Terui. *J Invest Dermatol*, **2011**, 131 : 1987.
12. A.E. Hargrove, T.F. Martinez, A.A. Hare, A.A. Kurmis, J.W. Phillips, S. Sud, K.J. Pienta, P.B. Dervan. *PLoS One*, **2015**, 10 : e0143161.
13. N.G. Nickols, P.B. Dervan. *Proc Natl Acad Sci U S A*,, **2007**, 104 : 10418.
14. K. Hiraoka, T. Inoue, R.D. Taylor, T. Watanabe, N. Koshikawa, H. Yoda, K. Shinohara, A. Takatori, H. Sugimoto, Y. Maru, T. Denda, K. Fujiwara, A. Balmain, T. Ozaki, T. Bando, H. Sugiyama, H. Nagase. *Nat Commun*, **2015**, 6 : 6706.
15. J.A. Raskatov, J.W. Puckett, P.B. Dervan. *Bioorg Med Chem*, **2014**, 22 : 4371.
16. K. Morita, K. Suzuki, S. Maeda, A. Matsuo, Y. Mitsuda, C. Tokushige, G. Kashiwazaki, J. Taniguchi, R. Maeda, M. Noura, M. Hirata, T. Kataoka, A. Yano, Y. Yamada, H. Kiyose, M. Tokumasu, H. Matsuo, S. Tanaka, Y. Okuno, M. Muto, K. Naka, K. Ito, T. Kitamura, Y. Kaneda, P.P. Liu, T. Bando, S. Adachi, H. Sugiyama, Y. Kamikubo. *J Clin Invest*, **2017**, 127 : 2815.
17. H. Matsuda, N. Fukuda, T. Ueno, Y. Tahira, H. Ayame, W. Zhang, T. Bando, H. Sugiyama, S. Saito, K. Matsumoto, H. Mugishima, K. Serie. *J Am Soc Nephrol*, **2006**, 17 : 422.

18. A. Fukasawa, T. Aoyama, T. Nagashima, N. Fukuda, T. Ueno, H. Sugiyama, H. Nagase, Y. Matsumoto. *Biopharm Drug Disp*, **2009**, 30 : 81.
19. T. Kamei, T. Aoyama, C. Tanaka, T. Nagashima, Y. Aoyama, H. Hayashi, H. Nagase, T. Ueno, N. Fukuda, Y. Matsumoto. *J Biomed Biotechnol*, **2012**, 2012 : 715928.
20. T.P. Best, B.S. Edelson, N.G. Nickols, P.B. Dervan. *Proc Natl Acad Sci U S A*, **2003**, 100 : 12063.
21. J.W. Trauger, E.E. Baird, M. Mrksich, P.B. Dervan. *J Am Chem Soc*, **1996**, 118 : 6160.
22. T. Watanabe, K. Shinohara, Y. Shinozaki, S. Uekusa, X. Wang, N. Koshikawa, K. Hiraoka, T. Inoue, J. Lin, T. Bando, H. Nagase. *Adv Tech Biol Med*, **2016**, 4 : 2.
23. K. Valko. *J Chromatography. A*, **2004**, 1037 : 299.
24. S. Nishijima, K. Shinohara, T. Bando, M. Minoshima, G. Kashiwazaki, H. Sugiyama. *Bioorg Med Chemistry*, **2010**, 18 : 978.
25. M.H. Abraham, C. Treiner, M. Roses, C. Rafols, Y. Ishihama. *J Chromatography A*, **1996**, 752 : 243.
26. B. Yang, H. Liu, J. Chen, M. Guan, H. Qiu. *J Chromatography A*, **2016**, 1468 : 79.
27. M.S. Blackledge, C. Melander. *Bioorg Med Chem*, **2013**, 21 : 6101.
28. M. Raica, A.M. Cimpean, D. Ribatti. *Eur J Cancer*, **2009**, 45 : 1924.
29. J.A. Raskatov, J.O. Szablowski, P.B. Dervan. *J Med Chem*, **2014**, 57 : 8471.
30. H. Hashizume, P. Baluk, S. Morikawa, J.W. McLean, G. Thurston, S. Roberge, R.K. Jain, D.M. McDonald. *Am J Pathol*, **2000**, 156 : 1363.
31. Y. Matsumura, H. Maeda. *Cancer Res*, **1986**, 46 : 6387.
32. H. Maeda, H. Nakamura, J. Fang. *Adv Drug Delivery Rev*, **2013**, 65 : 71.
33. D.M. Chenoweth, D.A. Harki, J.W. Phillips, C. Dose, P.B. Dervan. *J Am Chem Soc*, **2009**, 131 : 7182.
34. I. Nakase, N.B. Kobayashi, T. Takatani-Nakase, T. Yoshida. *Scientific Reports*, **2015**, 5 : 10300.
35. D.A. Harki, N. Satyamurthy, D.B. Stout, M.E. Phelps, P.B. Dervan. *Proc Natl Acad Sci U S A*, **2008**, 105 : 13039.
36. T.W. Synold, B. Xi, J. Wu, Y. Yen, B.C. Li, F. Yang, J.W. Phillips, N.G. Nickols, P.B. Dervan. *Cancer Chemo Pharmacol*, **2012**, 70 : 617.
37. A.E. Hargrove, J.A. Raskatov, J.L. Meier, D.C. Montgomery, P.B. Dervan. *J Med Chem*, **2012**, 55 : 5425.
38. T. Takagaki, T. Bando, M. Kitano, K. Hashiya, G. Kashiwazaki, H. Sugiyama. *Bioorg Med Chem*, **2011**, 19 : 5896.

39. T. Bando, H. Sugiyama. *Acc Chem Res*, **2006**, 39 : 935.
40. K. Valko, C.M. Du, C.D. Bevan, D.P. Reynolds, M.H. Abraham. *J Pharm Sci*, **2000**, 89 : 1085.
41. K. Iwase, K. Komatsu, S. Hirono, S. Nakagawa, I. Moriguchi. *Chem Pharma Bul*, **1985**, 33 : 2114.
42. K. Valkó, C. Bevan, D. Reynolds. *Anal Chem*, **1997**, 69 : 2022.
43. W.-C. Sun, K.R. Gee, D.H. Klaubert, R.P. Haugland. *J Org Chem*, **1997**, 62 : 6469.

9. Appendices

Table 1. Partition coefficients (logP_{OW}) and fluorescence quantum yield (ϕ_f^a) of compounds 1-5.

Compound	retention time (min)	logP_{OW}	ϕ_f^a
1	11.73	1.50	0.022
2	11.40	1.46	0.026
3	10.97	1.42	0.027
4	10.48	1.36	0.010
5	8.86	1.19	0.014

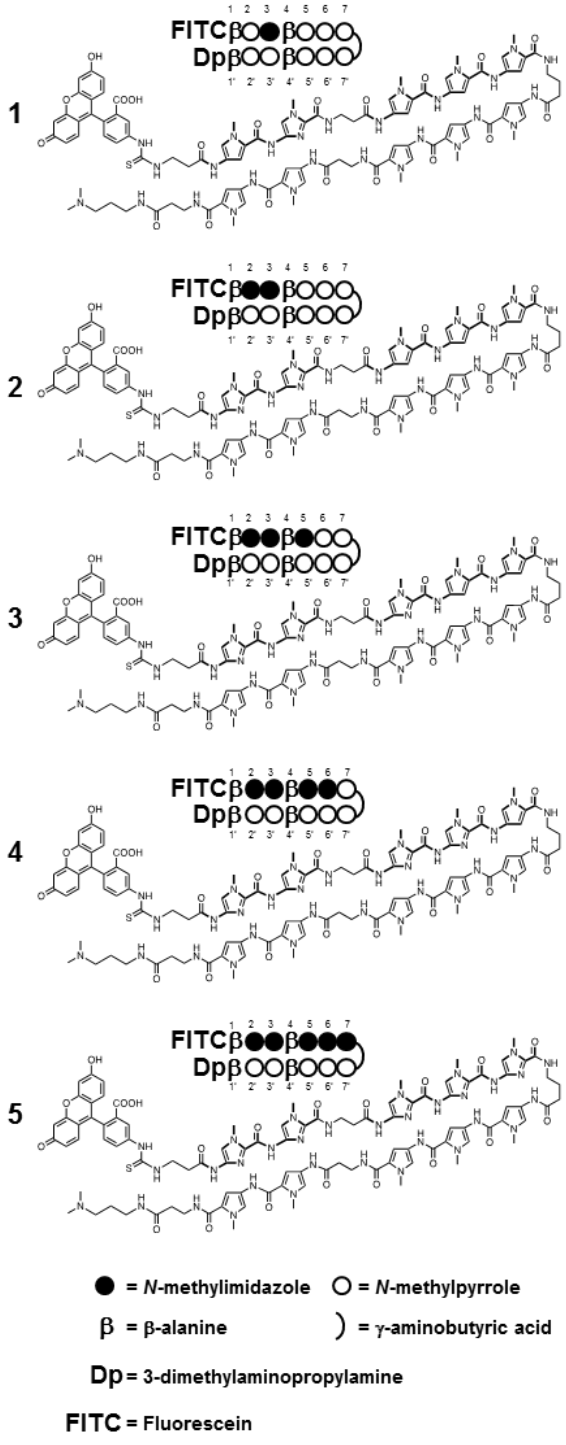

Figure 1. Chemical structures and graphical schemas of the pyrrole-imidazole polyamide-fluorescein conjugates 1-5 employed in this study

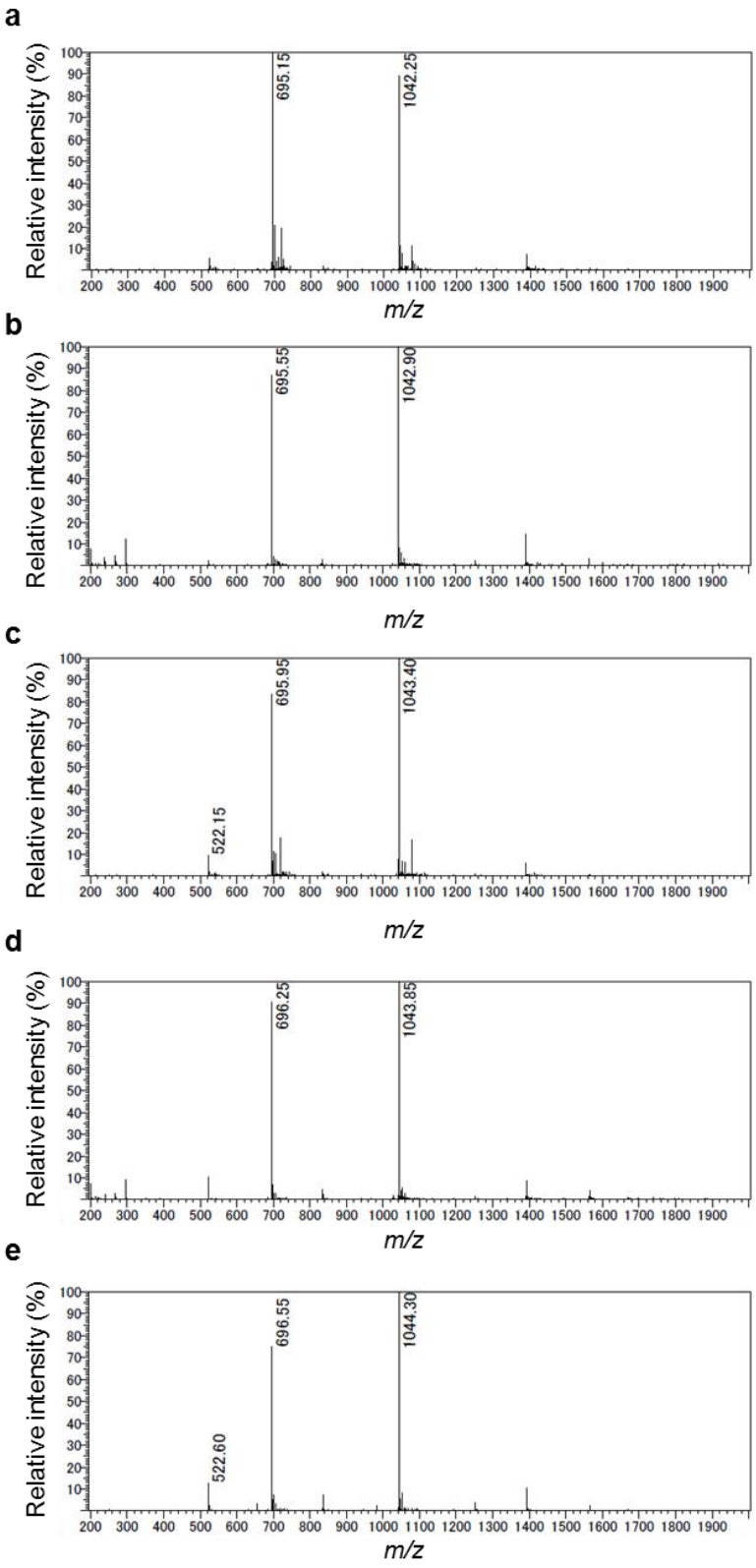

Figure 2. LC MS analysis of compuonds 1-5

MS spectra of compounds **1** (a), **2** (b), **3** (c), **4** (d), and **5** (e).

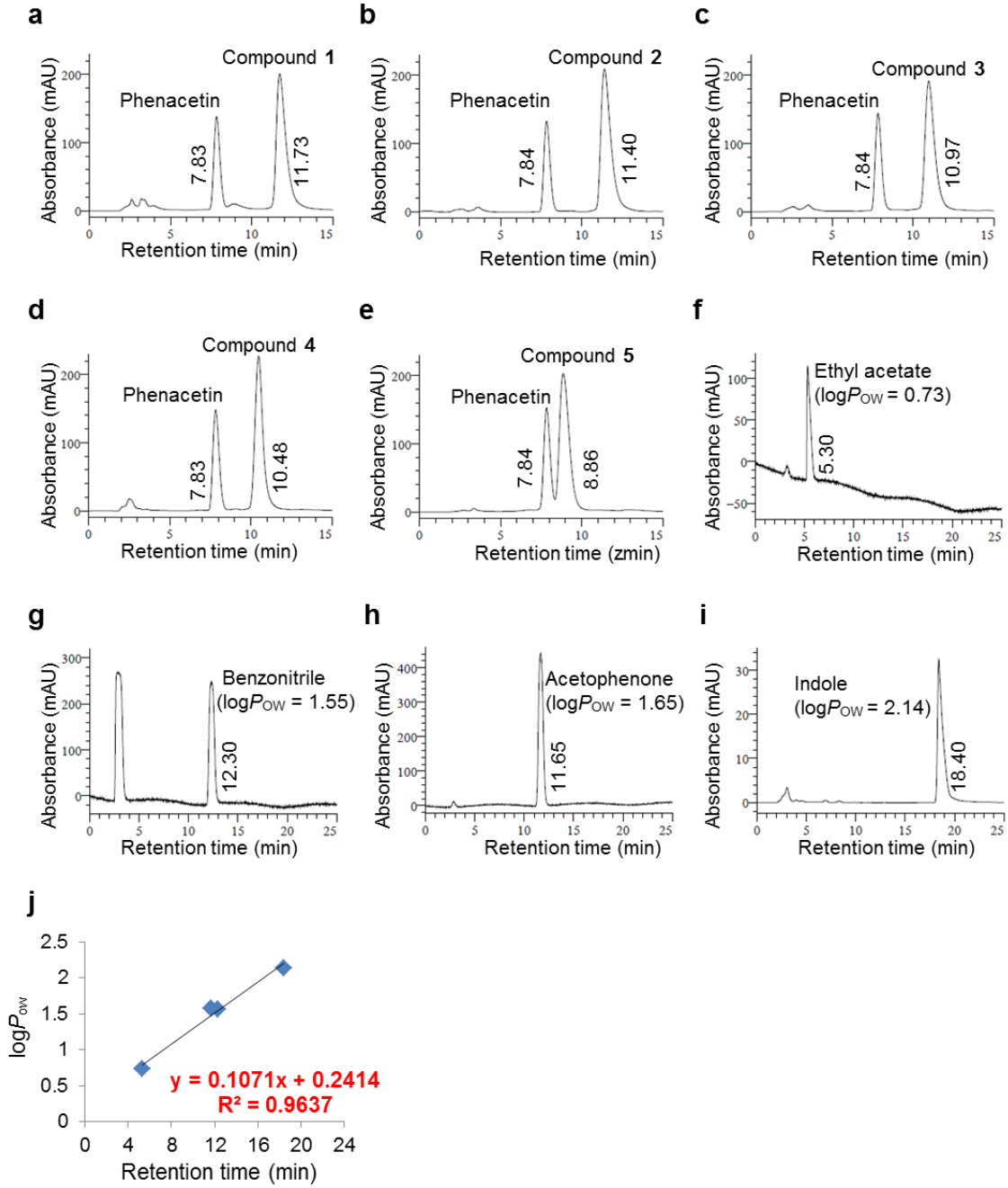

Figure 3. Chromatograms of compounds 1-5 and reference compounds

Chromatograms of indicated compounds were obtained by high pressure liquid chromatography and their retention times were shown: compounds **1** (a), **2** (b), **3** (c), **4** (d), **5** (e), ethyl acetate (f), benzonitrile (g), acetophenone (h), and indole (i). Phenacetin is used as an internal standard for compounds **1-5**. A standard curve was plotted for the retention times and the logP_{OW} values (j).

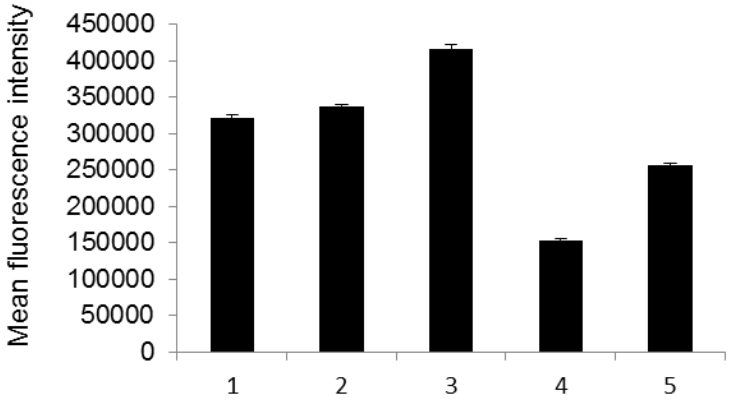

Figure 4. Fluorescence of compounds 1-5

10 μM of compounds 1-5 were incubated with the 100 μL of DMSO/PBS solution (1% v/v) at 37 °C. Sixty minutes after the incubation, their fluorescence intensities were measured by an ARVO X3 fluorescence spectrometer (PerkinElmer, MA, USA). Data shows mean ± SD of independent three experiments.

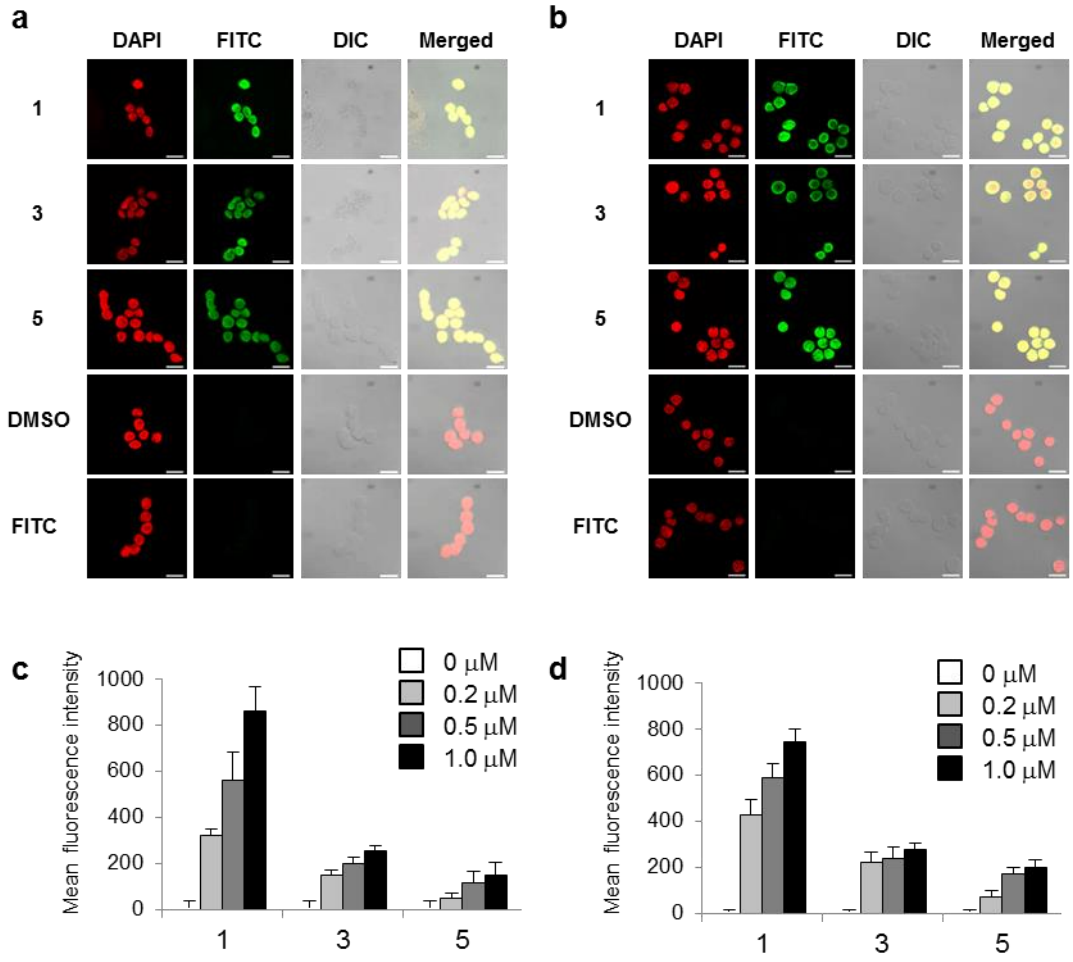

Figure 5. Nuclear uptake and fluorescence intensity of compounds 1, 3, and 5 in colon cancer cells

(a and b) Human colon cancer LS180 (a) and SW480 (b) cells were treated with PI polyamide-fluorescein conjugates **1**, **3**, **5**, FITC, or DMSO. Cells were stained with DAPI and images shown are captured under confocal laser microscopy (magnitude: x 630), with scale bars indicating 20 μm. (c and d) LS180 (c) and SW480 (d) cells were treated with compound **1**, **3**, or **5** at the indicated doses or left untreated for 24 hours at 37 °C. The fluorescence of these cells was determined by fluorospectrometer. Data show mean ± SD of triplicate samples.

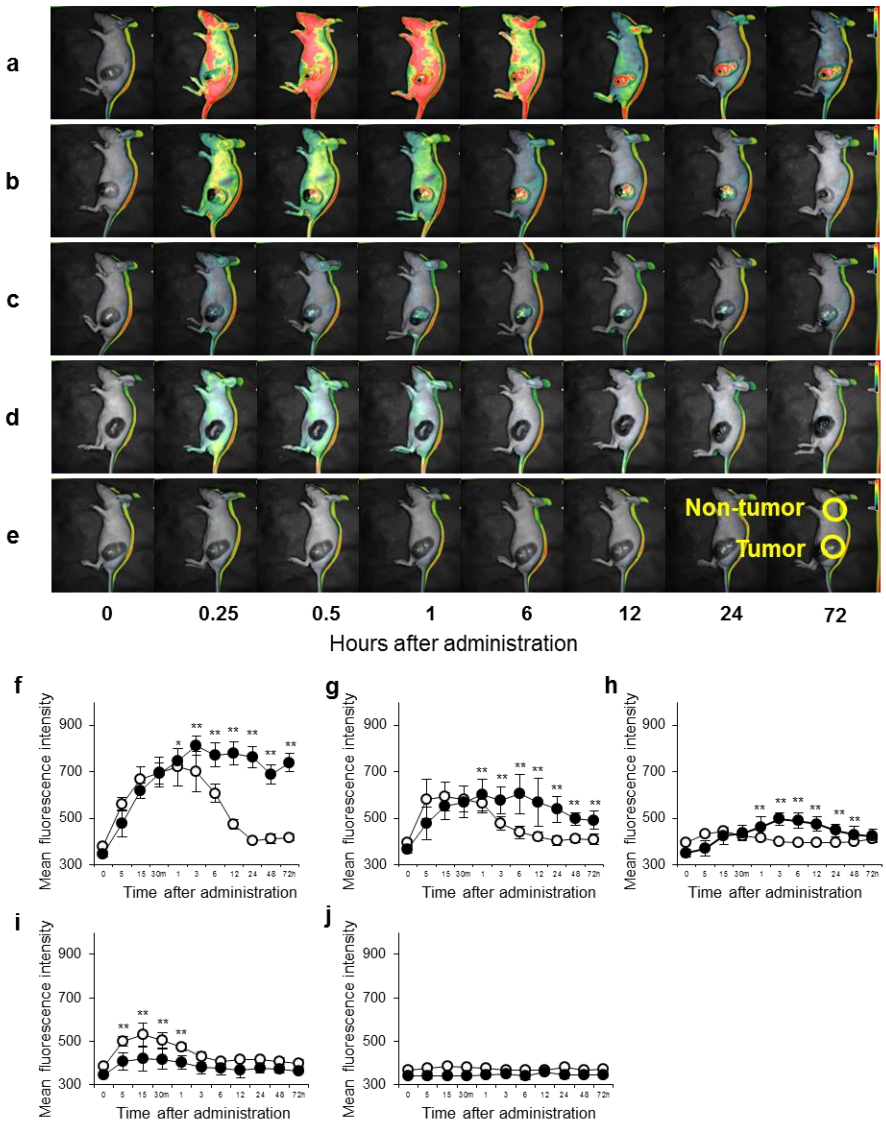

Figure 6. Representative images of 1, 3, and 5-treated mice and their mean fluorescein intensities of tumor and non-tumor areas

Human colon cancer LS180 cells were subcutaneously inoculated into flanks of nude mice. Compounds **1** (a), **3** (b), **5** (c), FITC (d), or 1.25% DMSO/PBS (e) was intravenously administrated into the tumor-bearing mice (1 mg/kg) upon approximately 1 cm of growth for *in vivo* fluorescent imaging. The fluorescence images of whole bodies of the treated mice were then taken by an *in vivo* imaging system at the indicated time points post-administration. Circles mark the tumor and the non-tumor areas for measuring fluorescein intensity. The mean fluorescent intensities at the tumor (closed circles) and at the non-tumor area (open circles) of tumor-bearing mice inoculated with compounds 1 (f), 3 (g), 5 (h), FITC (i), and DMSO (j) are shown; error bars indicate SD (n = 3, *$p < 0.05$, **$p < 0.01$).

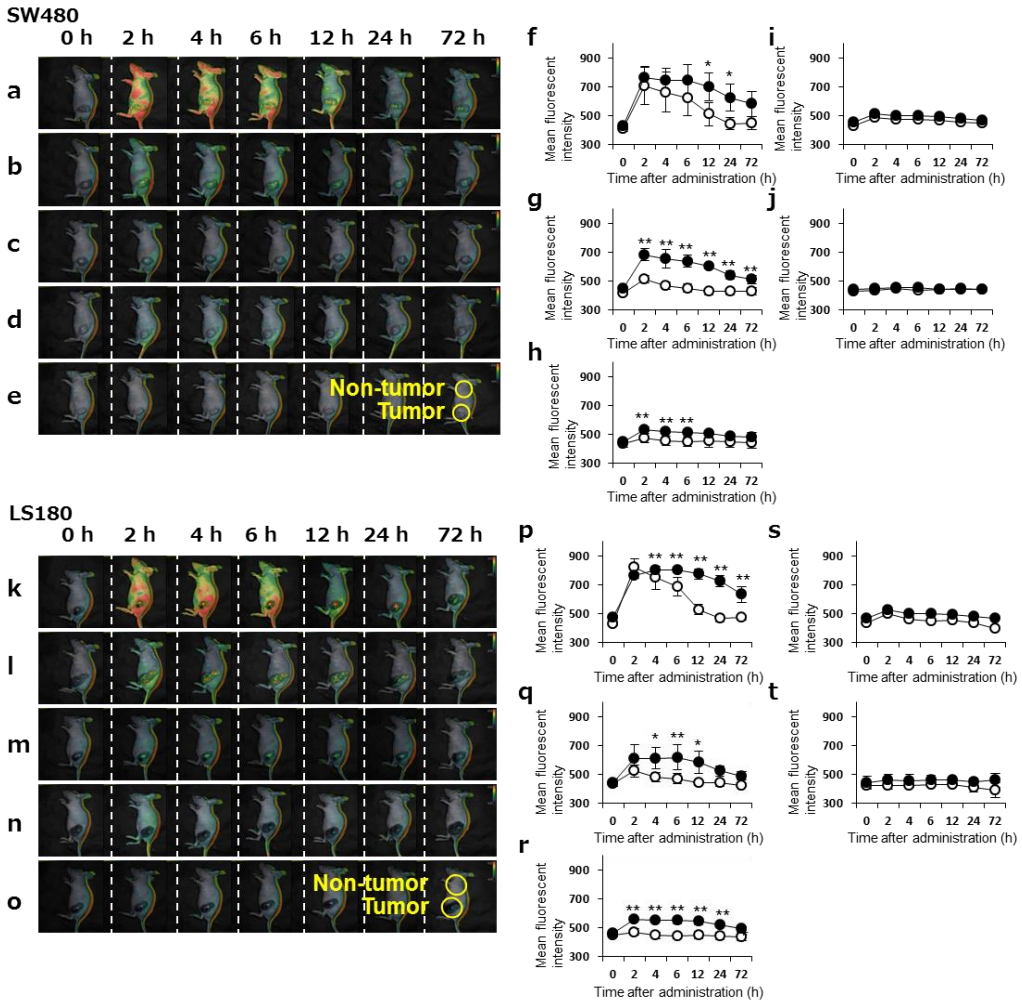

Figure 7. The biodistribution of PI polyamides in tissue sections prepared from PI polyamide-treated mice

Human colon cancer SW480 (5 x 10^6 cells/mouse, a-j) or LS180 (3 x 10^6 cells/mouse, k-t) cells were subcutaneously inoculated into flanks of nude mice. Either compound **1** (a, k), **3** (b, l), **5** (c, m), FITC (d, n), or 1.25% DMSO/PBS (e, o) was intravenously administrated into the tumor-bearing mice (n = 3) when the long diameter of xenograft tumors reaches approximate 1 cm. The fluorescence images of their entire bodies were then taken by an *in vivo* imaging system at the indicated time points post-administration. Representative images are shown and circles in the images are indicated as tumor and non-tumor areas for measurement of fluorescein intensity. The mean fluorescent intensities at tumor (closed circles) and at non-tumor skin area (open circles) of tumor-bearing mice inoculated with compounds 1 (f, p), 2 (g, q), 3 (h, r), FITC (I, s), and DMSO (j, t) are shown; error bars indicate SD (n = 3, $*p < 0.05$, $**p < 0.01$).

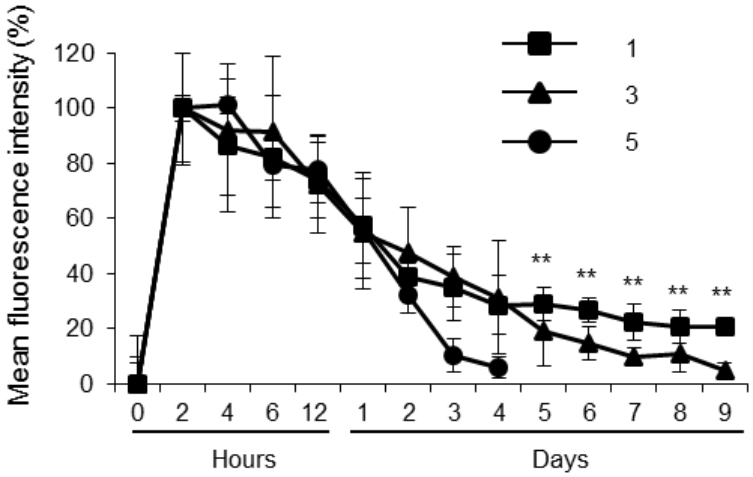

Figure 8. Percent of mean fluorescence intensities at tumor areas was measured for 9 days after administration

Human colon cancer LS180 cells were subcutaneously inoculated into flanks of nude mice. All injections were performed intravenously (1 mg/kg) upon approximately 1 cm of growth. Mice with the PI polyamide-fluorescein conjugate **1** (closed squares), **3** (closed triangles) and **5** (closed circles) were monitored at the indicated time points post-administration. The fluorescence intensity at 0 hours (before administration) and 2 hours was taken for 0% and 100%, respectively. Results show mean ± SD (n = 3 mice per group, $^{**}p < 0.01$).

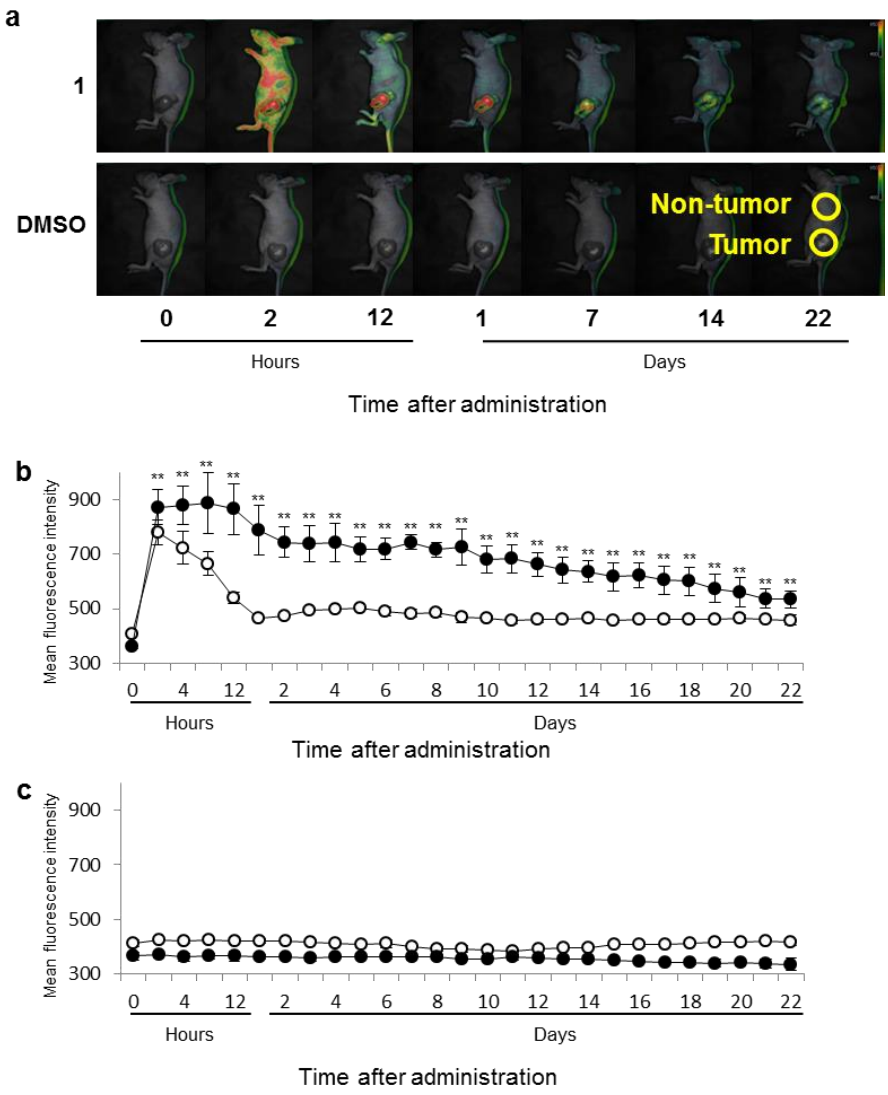

Figure 9. The bio-distribution of PI polyamides in tissue sections prepared from PI polyamide-treated mice

(a) Human colon cancer-derived SW480 cells (5 x 10^6 cells per mouse) were subcutaneously inoculated into left flanks of 5- to 8-weeks female BALB/c nude mice (Oriental Yeast, Tokyo, Japan). Compound **1** (1 mg/kg) or 1.25% DMSO/PBS was intravenously administrated into the tumor-bearing mice when the long diameter of xenograft tumors reaches about 1 cm, and these mice were monitored at the indicated time points post-administration. Circles mark the tumor and the non-tumor areas for measuring fluorescein intensity. (b and c) The mean fluorescent intensities at the tumor (closed circles) and at the non-tumor area (open circles) of mice with compounds 1 (b) or 1.25% DMSO/PBS (c) are shown. Results show mean ± SD (n = 3 mice per group, $^{**}p < 0.01$).

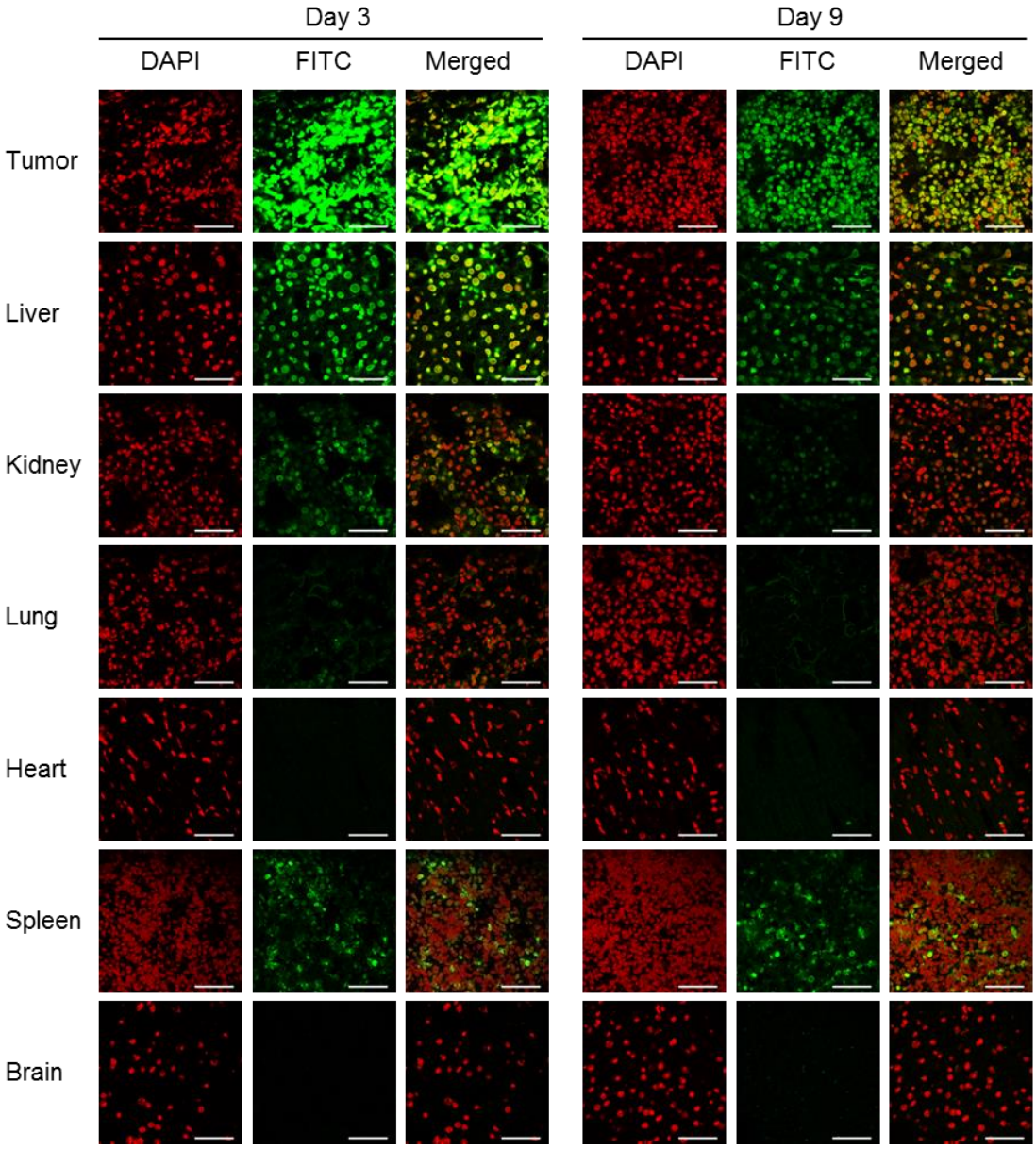

Figure 10. The fluorescent image of tissue sections prepared from compound 1-treated mice

Human colon cancer-derived LS180 cells (3 x 10^6 cells per mouse) were subcutaneously inoculated into left flanks of 5- to 8-weeks female BALB/c nude mice (Oriental Yeast, Tokyo, Japan). Compound **1** (1 mg/kg) was intravenously administrated into the tumor-bearing mice when the long diameter of xenograft tumors reaches about 1 cm. The mice were sacrificed at 3 days or 9 days after administration and then tumor, liver, kidney, heat, lung, spleen, and brain were resected. Frozen sections were prepared and observed under a DMI 4000B confocal laser microscope (Leica Microsystems, Wetzlar, Germany). Bars indicate 50 μm.

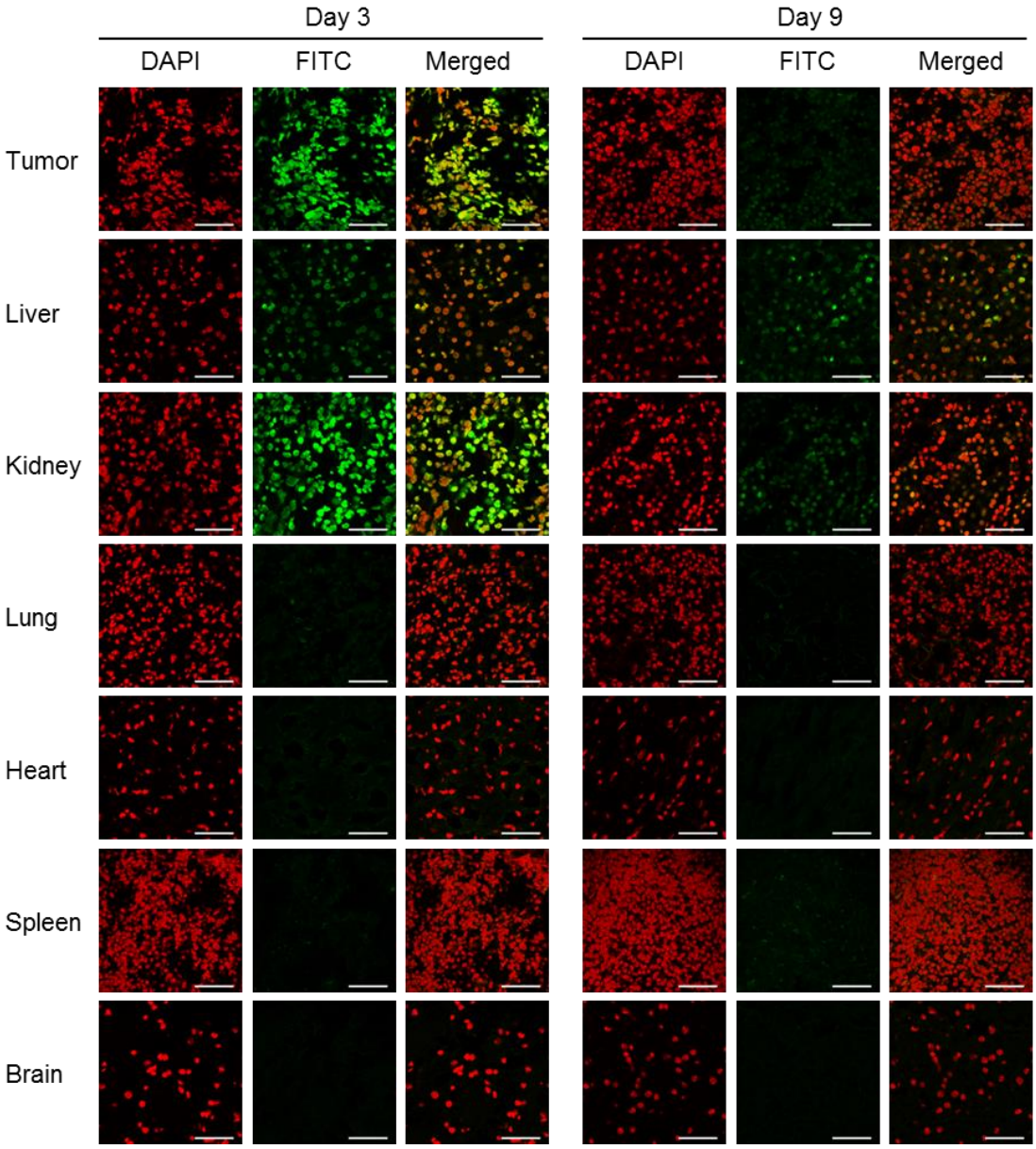

Figure 11. The fluorescent image of tissue sections prepared from compound 3-treated mice

Human colon cancer-derived LS180 cells (3 x 10^6 cells per mouse) were subcutaneously inoculated into left flanks of 5- to 8-weeks female BALB/c nude mice (Oriental Yeast, Tokyo, Japan). Compound **2** (1 mg/kg) was intravenously administrated into the tumor-bearing mice when the long diameter of xenograft tumors reaches about 1 cm. The mice were sacrificed at 3 days or 9 days after administration and then tumor, liver, kidney, heat, lung, spleen, and brain were resected. Frozen sections were prepared and observed under a DMI 4000B confocal laser microscope (Leica Microsystems, Wetzlar, Germany). Bars indicate 50 μm.

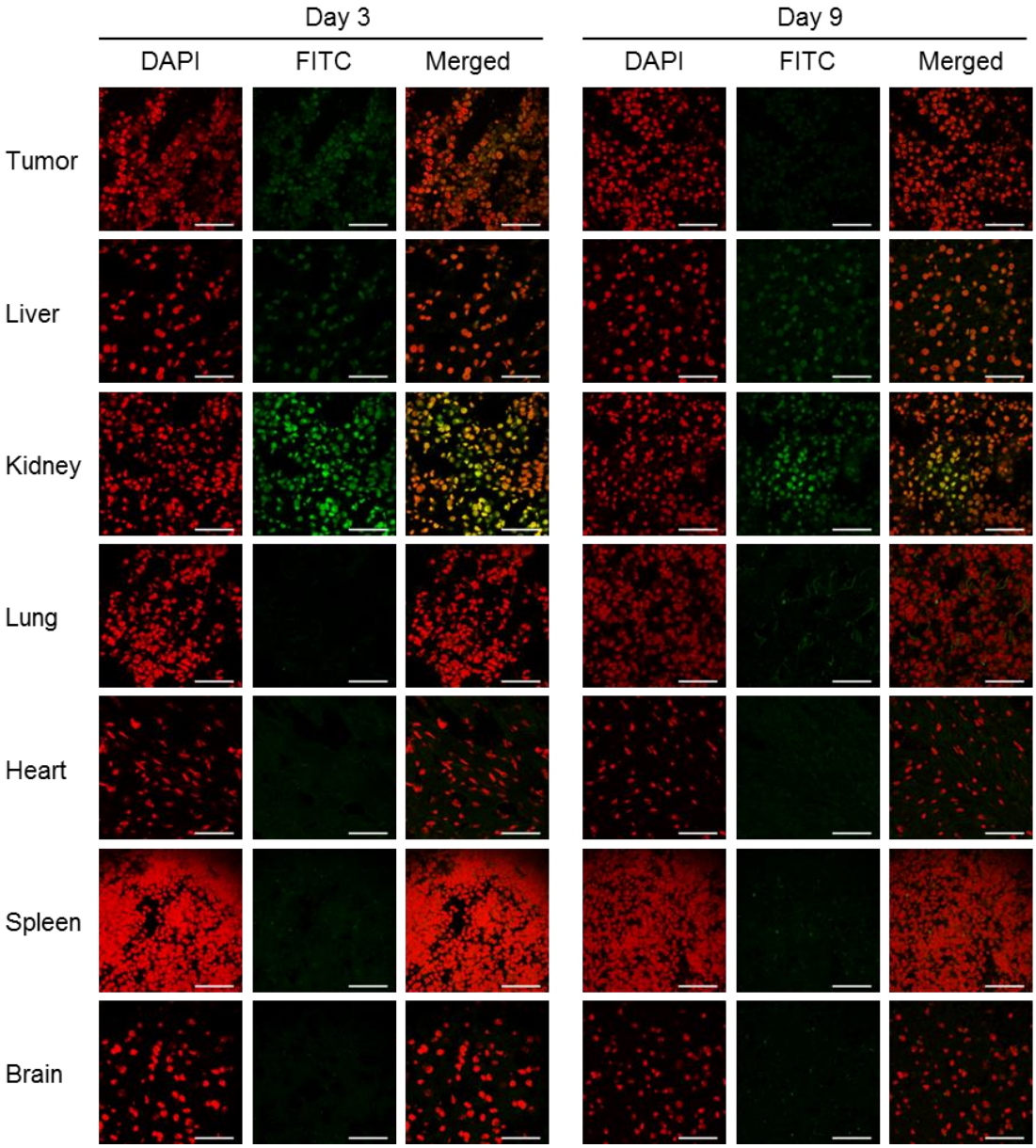

Figure 12. The fluorescent image of tissue sections prepared from compound 5-treated mice

Human colon cancer-derived LS180 cells (3 x 10^6 cells per mouse) were subcutaneously inoculated into left flanks of 5- to 8-weeks female BALB/c nude mice (Oriental Yeast, Tokyo, Japan). Compound **3** (1 mg/kg) was intravenously administrated into the tumor-bearing mice when the long diameter of xenograft tumors reaches about 1 cm. The mice were sacrificed at 3 days or 9 days after administration and then tumor, liver, kidney, heat, lung, spleen, and brain were resected. Frozen sections were prepared and observed under a DMI 4000B confocal laser microscope (Leica Microsystems, Wetzlar, Germany). Bars indicate 50 μm.

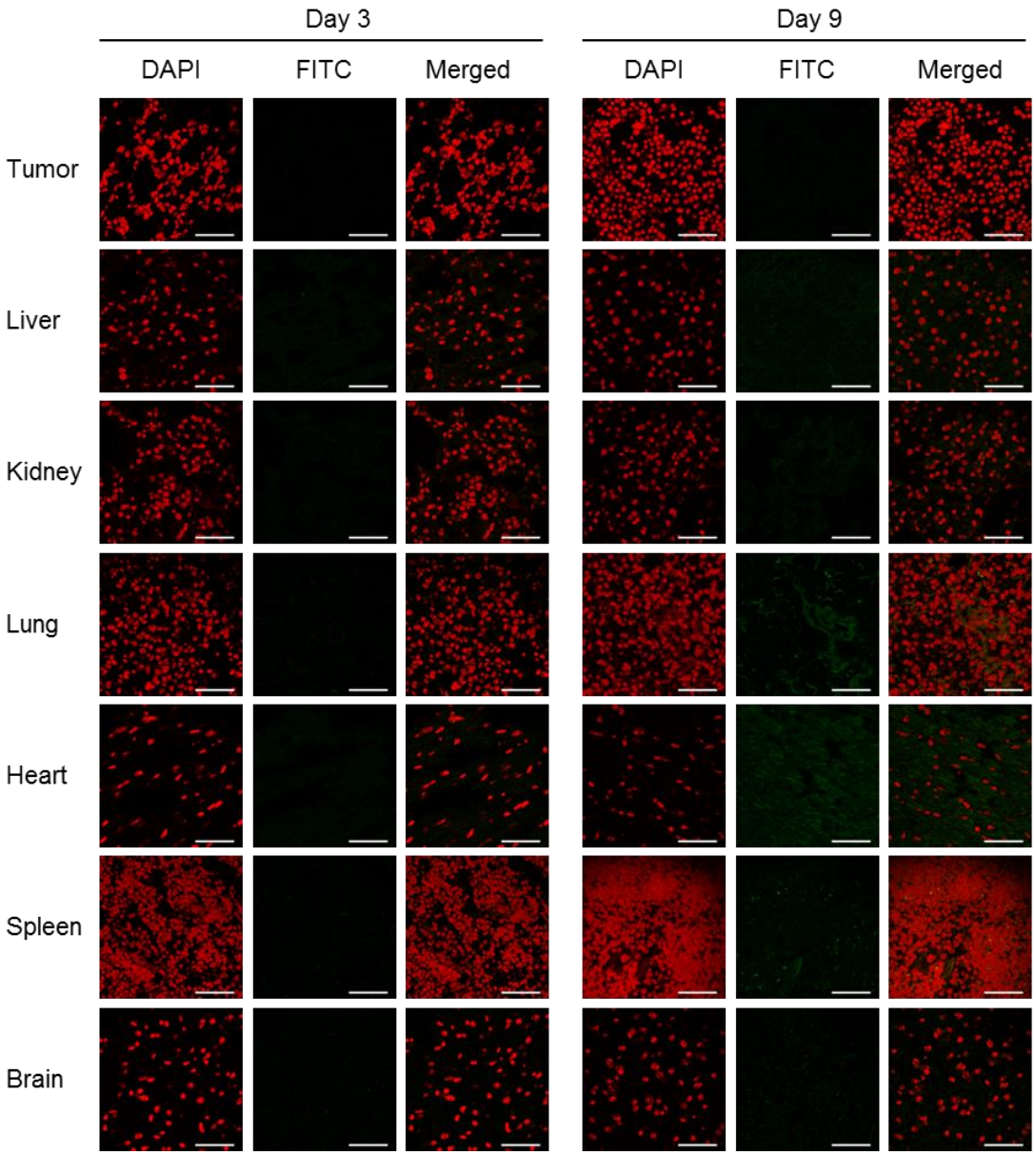

Figure 13. The fluorescent image of tissue sections prepared from DMSO-treated mice

Human colon cancer-derived LS180 cells (3 x 10^6 cells per mouse) were subcutaneously inoculated into left flanks of 5- to 8-weeks female BALB/c nude mice (Oriental Yeast, Tokyo, Japan). DMSO/PBS (1.25%, v/v) was intravenously administrated into the tumor-bearing mice when the long diameter of xenograft tumors reaches about 1 cm. The mice were sacrificed at 3 days or 9 days after administration and then tumor, liver, kidney, heat, lung, spleen, and brain were resected. Frozen sections were prepared and observed under a DMI 4000B confocal laser microscope (Leica Microsystems, Wetzlar, Germany). Bars indicate 50 μm.

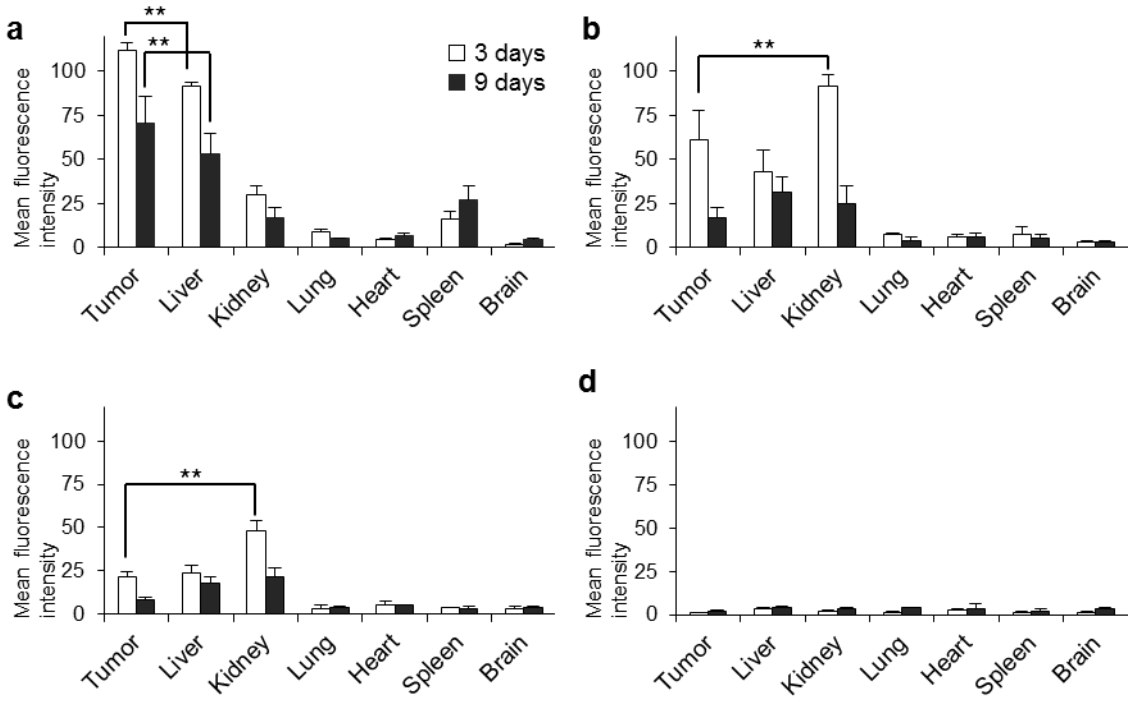

Figure 14. Fluorescein intensities of tumors and indicated organs from 1, 3, or 5-treated mice (3 and 9 days)

Tissue sections of tumors and various organs were prepared from LS180-derived tumor-bearing mice with the PI polyamide-fluorescein conjugates **1** (a), **3** (b), **5** (c), or DMSO (d) as a vehicle control at 3 days and 9 days post administration. Their fluorescence was captured under a confocal laser microscope and quantitated their fluorescence intensity. Data shows mean ± SD, n = 3 mice per group, $^{**}p < 0.01$.

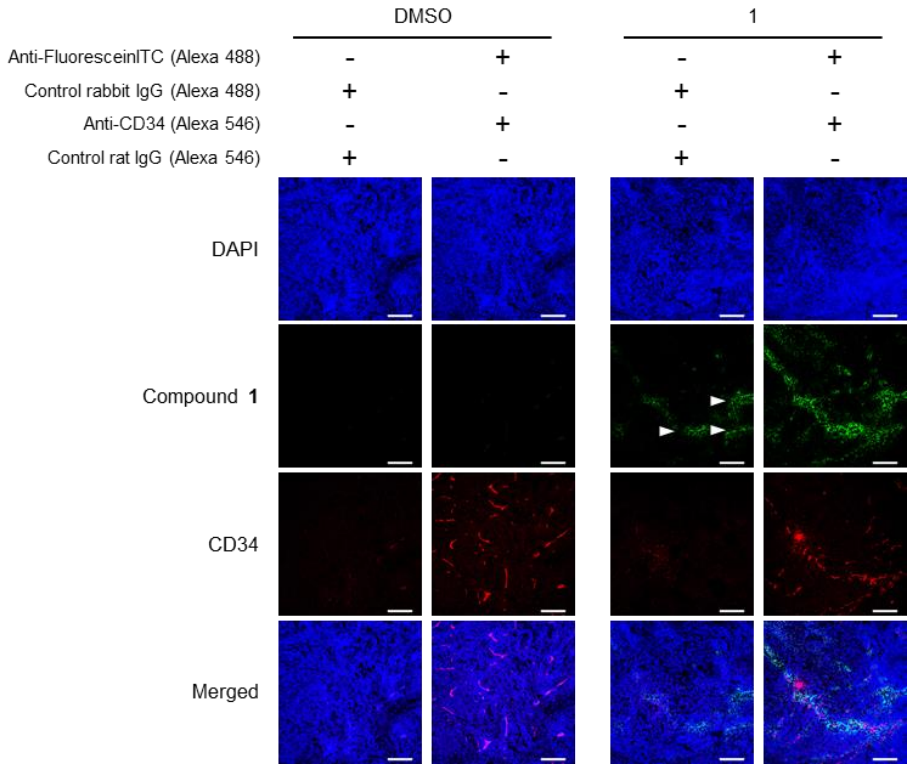

Figure 15. Distribution of compound 1 along with tumor blood vessels

Human colon cancer-derived LS180 cells (3 x 10^6 cells per mouse) were subcutaneously inoculated into left flanks of 5- to 8-weeks female BALB/c nude mice (Oriental Yeast, Tokyo, Japan). Compound **1** (1 mg/kg) was intravenously administrated into the tumor-bearing mice when the long diameter of xenograft tumors reaches about 1 cm. Mice were sacrificed at 3 days after administration. Tumor tissues were fixed in 4% paraformaldehyde (Nacalai tesque, Kyoto, Japan) for 16 hours at 4 °C and embedded in paraffin (Leica biosystems, Eisfeld, Germany). The paraffin-embedded sections were deparaffinized in 10 mM citrate buffer (pH 6.0) for 10 min at 90 °C. After blocking of nonspecific reactivity with blocking buffer (Protein Block Serum-Free; DAKO, Tokyo, Japan), tissue sections were incubated with primary antibodies against fluorescein (x 100, Abcam, Cambridge, UK), murine CD34 (x 250, Novus Biologicals, Littleton, CO, USA), or respective control rat or rabbit IgG (Immuno-Biological Laboratories Co, Ltd.),) for 16 hoursat 4 °C, followed by incubation with secondary antibodies Alexa488-conjugated anti-rabbit IgG (x 500, Invitrogen, Carlsbad, CA, USA) and Alexa546-conjugated anti-rat IgG (x 500, Invitrogen) for 1 hours at room temperature. Sections were mounted with VECTASHIELD Mounting Medium with DAPI (Vector Laboratory, Burlingame, CA, USA) and visualized under a DMI6000 CS microscope (Leica Microsystems, Wetzlar, Germany). Compound 1 in tumor tissue is preferentially distributed along with CD34-positive blood vessels. Arrows indicate fluorescence from residual compound 1. Bars indicate 200 µm.

Title: Hydrophobic structure of hairpin ten-ring pyrrole-imidazole polyamides enhances tumor tissue accumulation/retention in vivo.

Author: Takahiro Inoue,Osamu Shimozato,Nina Matsuo,Yusuke Mori,Yoshinao Shinozaki,Jason Lin,Takayoshi Watanabe,Atsushi Takatori,Nobuko Koshikawa,Toshinori Ozaki,Hiroki Nagase

Publication: Bioorganic & Medicinal Chemistry

Publisher: Elsevier

Date: Available online 19 March 2018

Journal: Bioorganic & Medicinal Chemistry

Hydrophobic structure of hairpin ten-ring pyrrole-imidazole polyamides enhances tumor tissue accumulation/retention *in vivo*.

Takahiro Inoue, Osamu Shimozato, Nina Matsuo, Yusuke Mori, Yoshinao Shinozaki, Jason Lin, Takayoshi Watanabe, Atsushi Takatori, Nobuko Koshikawa, Toshinori Ozaki, Hiroki Nagase

DOI : https://doi.org/10.1016/j.bmc.2018.03.029

平成 30 年 3 月 19 日　印刷中